PHILOSOPHICAL TRANSACTIONS OF THE ROYAL SOCIETY A

rsta.royalsocietypublishing.org

Research

Cite this article: Albertini, C, Cadoni, E, Solomos, G. 2014 Advances in the Hopkinson bar testing of irradiated/non-irradiated nuclear materials and large specimens. *Phil. Trans. R. Soc. A* **372**: 20130197.
http://dx.doi.org/10.1098/rsta.2013.0197

One contribution of 12 to a Theme Issue 'Shock and blast: celebrating the centenary of Bertram Hopkinson's seminal paper of 1914 (Part 1)'.

Subject Areas:
materials science, mechanical engineering, power and energy systems, structural engineering

Keywords:
irradiated nuclear material, high strain rate, tension, large Hopkinson bar

Author for correspondence:
Ezio Cadoni
e-mail: ezio.cadoni@supsi.ch

Advances in the Hopkinson bar testing of irradiated/non-irradiated nuclear materials and large specimens

Carlo Albertini[1], Ezio Cadoni[2] and George Solomos[1]

[1]European Commission, Joint Research Centre, IPSC, Ispra 21027, Italy
[2]DynaMat Lab, University of Applied Sciences of Southern Switzerland, Canobbio 6952, Switzerland

A brief review of the technological advances of the Hopkinson bar technique in tension for the study of irradiated/non-irradiated nuclear materials and the development of this technology for large specimens is presented. Comparisons are made of the dynamic behaviour of non-irradiated and irradiated materials previously subjected to creep, low cycle fatigue and irradiation (2, 10 and 30 displacements per atom). In particular, complete results of the effect of irradiation on the dynamic mechanical properties of AISI304L steel, tested at 20, 400 and 550°C are presented. These high strain rate tests have been performed with a modified Hopkinson bar (MHB), installed inside a hot cell. Examples of testing large nuclear steel specimens with a very large Hopkinson bar are also shown. The results overall demonstrate the capability of the MHB to efficiently reproduce the material stress conditions in case of accidental internal and external dynamic loadings in nuclear reactors, thus contributing to the important process of their structural assessment.

1. Introduction

Starting from the early 1970s until the end of the twentieth century, research activity in the nuclear field of the Joint Research Centre (JRC) was concentrated on problems of nuclear reactor safety, especially the assessment of the steel or reinforced concrete containment

Royal Society Publishing

structures of the different types of nuclear reactors: light water reactor, pressurized water reactor (PWR) and fast breeder reactor (FBR). Their mechanical resistance and integrity were of concern under hypothetical accidental dynamic loadings like those due to gas explosions or liquid over-pressure arising in case of malfunctioning of some reactor components (e.g. cooling system, reactivity control bars, etc.).

In particular, at JRC-Ispra, the steel pressure vessel directly housing the reactor core and the steel containment shell surrounding the reactor pressure vessel and other reactor components were considered. The assessment of their resistance was conducted by means of calculations with finite-element (FE) codes, where the constitutive equations in dynamics of the shell and the vessel steels would have to be implemented. The calibration of these constitutive equations should be based on the stress–strain curves in tension derived at high strain rates ranging between one and a few hundred strain per second.

In order to accomplish the above dynamic material testing programme for the high ductility nuclear steels, new impact testing rigs needed to be developed. They should be capable of generating strong and long duration pulses (from tens of microseconds to a few milliseconds) of constant amplitude, necessary for imposing to the steel specimens large displacements at constant speed and for leading them to fracture.

Two basic set-ups were initially developed:

— a hydro-pneumatic machine, working in tension, for strain rates from 1 to 100 s^{-1},
— a Hopkinson bar, appropriately modified for the generation of long duration pulses, for direct tension tests and for strain rates from 100 to 1000 s^{-1}.

Owing to the scope of this paper on the occasion of B. Hopkinson's centenary, only the original aspects of this new Hopkinson bar will be described here. With respect to the classical configurations [1–3], the main modification introduced in the new Hopkinson bar is the substitution of the impacting projectile bar, for the generation of the loading pulse, with an elastic steel bar, which is solidly connected to the incident (input) bar. As will be explained in the following, by statically pre-tensioning this bar and then suddenly releasing it by means of a special device, a loading pulse is generated and propagated down the input bar, as before.

The initial apparatus of this type included a pre-tensioned bar of 10 mm diameter and 6 m length, thus generating a pulse of 2.4 ms duration with a rise time of about 30 µs, sufficient to bring to rupture a ductile steel specimen of 3 mm diameter. Owing to the applied science character of the research conducted at the JRC, the new Hopkinson bar was patented in the years 1973–1974 [4]. The first results obtained with this modified Hopkinson bar (MHB) were published in the years 1974–1983 [5–8]. They concerned austenitic and ferritic virgin steels used in experiments of down-scaled reactor containment shell models subjected to explosion and served to validate numerical simulation predictions [8].

However, a more realistic assessment of the resistance of the containment shells required the implementation in the codes of the dynamic constitutive equations for these steels, representative of their damaged states owing to the environmental and loading conditions characteristic of the nuclear reactor functioning. For producing appropriate experimental data, the MHB was installed for the first time ever in the hot cell laboratory of the JRC-Ispra. This has allowed measurements to be made of the dynamic stress–strain curves at high temperatures (around 550°C) of austenitic stainless steels previously subjected to creep, low cycle fatigue and irradiation (up to 30 displacements per atom (dpa)). Most of the findings of this long-term research were published in a series of ASTM special publications [9–13] regarding properties of irradiated materials.

Owing to the fact that most of the above-mentioned research was performed using small steel specimens of 3 mm diameter and 5 mm gauge length, the issue of the size effect was naturally raised. An investigation of the specimen size effect on the dynamic material properties has been performed by means of a large MHB of the same type as that described above, which was constructed at JRC-Ispra in mid-1980s. The pre-tensioned and output bars each had a length of 100 m and a maximum pre-tension of 5 MN could be applied [14,15]. The generated tension

pulse was of maximum amplitude of 2.5 MN, of 40 ms duration and of about 50 µs rise time, and thus it has rendered possible the tensile testing of large specimens, having a diameter of 30 mm and gauge length of 50 mm, at strain rates between 20 and 250 s^{-1}. This has allowed comparison of the results with those of the small specimens and the efficient verification of the specimen size effect in dynamics (work performed in the frame of the European project REVISA [16]).

Finally, it is mentioned that the assessment of containment shells against accidental dynamic loading should also take into account the multi-axiality of the material stressing. This problem points to the need of verifying the material yield criteria in the dynamic regime, at least under biaxial loading. To this end, a biaxial version of the MHB was developed, consisting of four arms aligned 2 × 2 along two orthogonal axes and acting on a cruciform specimen [17,18].

All the applications mentioned above attest to the importance and impact that this MHB has had on the research in support of the structural safety assessment of nuclear reactors. Selected results of this long activity are presented in this paper, together with some fresh data concerning the dynamic material properties of the AISI304L austenitic stainless steel in its as-received and damaged states.

2. Dynamic response of materials and reactor safety

Nuclear reactor containment steel shells are designed to absorb through elasto-early plastic deformation the energy delivered by a hypothetical accident. Therefore, the ideal stress–strain–strain rate curves of the steel used for the shells should show not only high values of ultimate strength and fracture strain, but also strain hardening, strain rate hardening and large uniform strain (i.e. the strain corresponding to the ultimate strength). All these are characteristics assuring a stable plastic flow of the steel without the appearance of early localizations which could compromise the response of the shell structure. Normally at room temperature, the used austenitic and ferritic steels exhibit a dynamic flow curve close to the ideal one, as shown in figure 1 for AISI316H austenitic stainless steel.

In reality, nuclear reactor structures work at high temperatures, they are subjected to thermo-mechanical loading cycles causing fatigue and creep damage, and they are further damaged due to irradiation, corrosion, stress corrosion and multi-axial loading (this last one reducing their equivalent fracture strain [18]). Therefore, the capability of the containment shell to actually contain a hypothetical accident relies on damaged steels, whose elastic-plastic flow curves at high strain rate should, as much as possible, resemble the ideal stress–strain–strain rate curves described above. To check this fundamental point, a substantial number of tests were performed aiming to measure the dynamic mechanical properties of nuclear reactor structural materials both in as-received and in pre-damaged conditions (European Union Nuclear Fission Safety Programmes 1973–2000 'Containment analysis of severe accidents in nuclear reactors').

Austenitic stainless steels are characterized by a good resistance to general corrosion at elevated temperature. This has favoured their widespread use in primary and auxiliary circuits of PWRs and in the containment structures of FBRs, where they work at temperatures ranging from 400 to 550°C. Consequently, one family of materials investigated were the austenitic stainless steels (AISI316, AISI304 and AISI321), which were tested in uniaxial tension in a strain rate range of six orders of magnitude, from 10^{-3} to 10^{3} s^{-1}, and at temperatures of 20, 200 ÷ 900°C. These testing conditions should reproduce the loading and environmental conditions that are assumed to be encountered in a nuclear reactor in case of a severe accident.

The steel specimens have also been tested in conditions of pre-damage corresponding to those at the end-of-life of the reactor structures. In this case, the specimens, before impact testing, have been subjected to

— irradiation at increasing damage levels from 2 to 30 dpa,
— creep loading at a temperature of 550°C and at 0.4, 0.6, 0.8 of end-of-life time,
— different levels of temperature (RT, 300, 400, 550, 600, 700°C),

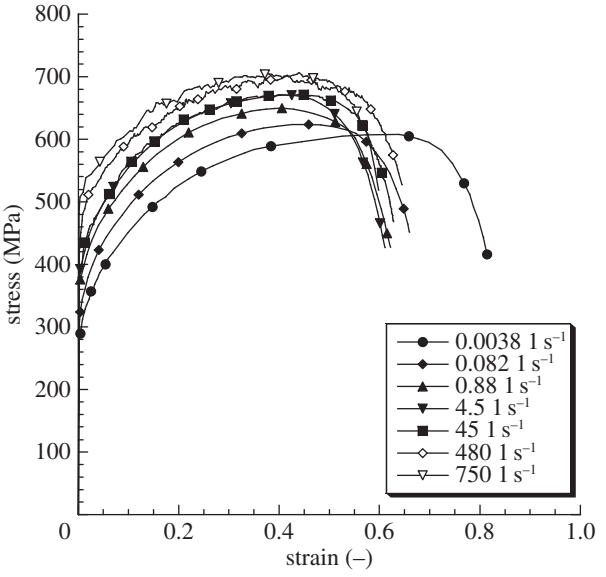

Figure 1. Stress–strain curves of AISI 316H stainless steel at different strain rates and at room temperature produced with 3-mm diameter specimens.

— thermal ageing effects for periods of 2000, 10 000, 50 000 h, and
— low cycle fatigue at different deformation levels (0.6 and 1%) and different cycle ratios (0.2, 0.4 and 0.6), temperature of 500°C and successive superposed irradiation of 2 dpa.

The above-described pre-damage conditions of the specimens can be considered as nearly equivalent to those exerted on the structural materials by the thermo-mechanical cycles and by the radiation which exist inside a nuclear reactor during its design service life.

The total number of specimens tested was approximately 1000. From each test, the corresponding stress–strain curve has been constructed and the most important parameters, such as yield stress, uniform strain and fracture strain, have been reported. The data obtained have been used to calibrate some viscoplastic constitutive equations (e.g. Perzyna, Bodner and Prandtl) implemented in the FE codes for the analysis of severe accidents effects on reactor structures.

3. The modified Hopkinson bar for tension testing

The development of the tension version of the MHB took place at the beginning of 1970s, as described in [5–7,19,20] and in the patents listed in [4]. Its schematic is presented in figure 2. As already introduced, the MHB consists of a pre-tensioned bar (substituting the projectile of the classical Hopkinson bar) and an incident (input) bar solidly connected together, and of a transmitter (output) bar and the specimen, inserted between the two last bars.

The MHB functioning is based on storing an amount of elastic mechanical energy in the pre-tensioned bar by statically tensioning it up to a certain stress (lower than its yield strength). To do this, the end section of the pre-tensioned bar contiguous to the incident bar is blocked by a brittle intermediate piece while the other end is pulled by means of a hydraulic actuator. Once the desired elastic energy in the pre-tensioned bar has been reached, the brittle intermediate piece is ruptured and the blockage is released. This gives rise to the contemporaneous generation of two elastic plane waves:

— An unloading wave, which starts from the bar section left free by the blockage and propagates along the pre-tensioned bar.

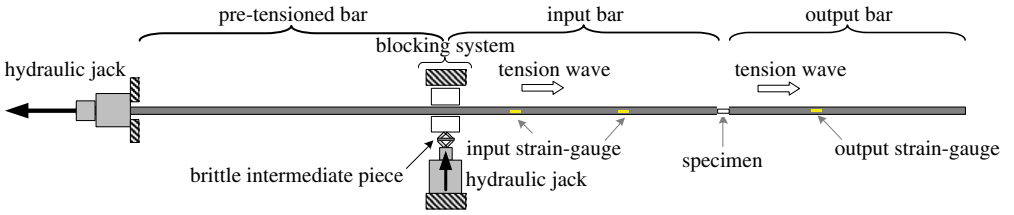

Figure 2. MHB with pre-tensioned bar loading device for tensile testing. (Online version in colour.)

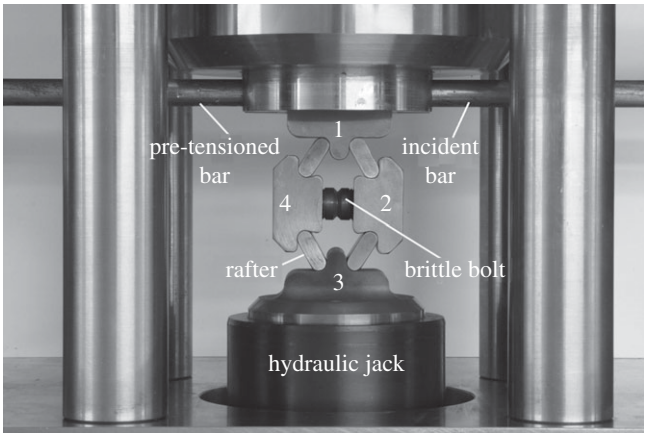

Figure 3. Blocking system called 'θ' theta clamp.

— A tension wave, which starts from the same bar section and propagates along the incident bar. This wave reaches and loads the specimen (until fracture), and it propagates to the transmitter bar, which it also loads in tension.

The duration of the tension pulse loading the specimen corresponds to the travel time of the unloading wave from the unblocked bar section to the hydraulic actuator and back. Thus, if L_p is the length of the pre-tensioned bar, the pulse duration would be $2L_p/C_0$, where $C_0 = \sqrt{(E/\rho)}$ is the fundamental bar wave velocity, $E =$ bar Young modulus and $\rho =$ bar material density. The amplitude of the generated tensile stress pulse is half that of the static stress value established in the pre-tensioned bar by the hydraulic actuator.

By using a rather long pre-tensioned bar, it is possible to generate a tensile pulse of long duration allowing the deformation until fracture of ductile specimens at medium–high strain rates. In this case, the use of a transmitter bar of length correspondent to that of the pre-tensioned bar (or the use of a momentum trap) is appropriate in order to deform the specimen under the clean and controlled loading resulting only from the incident tension pulse. Otherwise, the superposition of the wave reflections from the distal end of the transmitter bar would render very complicated and uncertain the analysis of the recorded signals. This last test condition is also fundamental for the success of the dynamic testing of fragile specimens, like those having been subjected to high irradiation doses.

A few words should be spent here for explaining how the brittle intermediate piece and the whole blocking mechanism, shown in figure 3, are designed and work. The system, also called the 'theta clamp' because of its resemblance to this Greek alphabet letter, has the shape of a parallelogram, whose sides (four metal rafter plates) are kept together by four supporting pieces 1-2-3-4, placed at the vertices of the parallelogram. One of these supporting pieces (3) is mounted

on a hydraulic jack and the diagonally opposite piece (1) is in contact with the end section of the pre-tensioned bar. The two other diagonally opposite pieces (2 and 4) are held together by a notched brittle bolt (screwed inside them).

As seen in figure 3, the hydraulic jack acting on the vertex 3 of the theta parallelogram exerts a transverse force (by compressing the sides of the parallelogram and stretching the notched brittle bolt) through piece 1 on the end section of the pre-tensioned bar, blocking it by friction against a curved anvil. The pre-tensioned bar can then be statically stretched to the desired level by pulling on its other end. At this point, the transverse hydraulic jack increases further the squeezing of the parallelogram 1-2-3-4 until the notched bolt fractures in a brittle manner provoking the 'explosive collapse' of the parallelogram.

The controlled collapse of the parallelogram is a key factor for assuring that

— the end section of the pre-tensioned bar is instantaneously left free, as needed for the generation of a tension pulse having a very short rise time (about 30 μs), and
— the end section of the pre-tensioned bar is left free in a clean manner without receiving unwanted transverse bending pulses, and therefore assuring that the tension wave propagating toward the specimen along the incident bar is an elastic plane wave without bending components.

The good functioning of this blocking system is crucial for the experimental success and validity of the MHB testing and, owing to its originality, the theta clamp has also been patented [21].

In the MHB, the bar diameter is small (e.g. 10 mm) in comparison with the wavelength of the generated tension pulse, which depends on the length of the pre-tensioned bar and can be of the order of some metres. Therefore, the conditions for the propagation of the generated elastic plane stress wave without dispersion and absorption along the incident and the transmitter bars, with velocity $C_0 = \sqrt{(E/\rho)}$, are amply attained. Under the well-substantiated assumption of specimen equilibrium, the engineering stress σ, strain rate $\mathrm{d}\varepsilon/\mathrm{d}t$ and strain ε of the specimen can simply be calculated from equations (3.1) [2,3]

$$\sigma(t) = E_\mathrm{b}\varepsilon_\mathrm{T}(t)\frac{A_\mathrm{b}}{A}, \quad \dot{\varepsilon}(t) = \frac{2C_0}{L}\varepsilon_\mathrm{R}(t) \quad \text{and} \quad \varepsilon(t) = \frac{2C_0}{L}\int_0^t \varepsilon_\mathrm{R}(z)\mathrm{d}z, \tag{3.1}$$

where, as usual, ε_T = transmitted pulse; ε_R = reflected pulse; E_b = bar Young modulus; A_b = bar cross-sectional area; A = specimen cross-sectional area; L = specimen gauge length. As is realized, owing to the long incident pulse ε_I, the reflected pulse ε_R cannot be isolated and recorded separately because, for practical reasons, the length of the incident bar is chosen shorter than that of the pre-tensioned bar. However, this is easily overcome by using two strain gauge stations on the incident bar, as shown in figure 2. The first of them captures mainly the ε_I signal and the second one (closer to the specimen) captures both the ε_I and the ε_R signals. By time shifting these two records to the same origin and then subtracting them, the ε_R record can be obtained.

(a) Some advantages of the modified tension Hopkinson bar

(1) The duration of the pulse can be increased to several milliseconds, as needed, without problems of vibrations or guidance, as in the case of a projectile shot by a gas-gun, by simply increasing the length of the pre-tensioned bar. In fact, at the JRC-Ispra, this length is 100 m, thus generating pulses of 40 ms. Long duration pulses are needed for the study of large deformations and fracture of highly ductile materials at strain rates in the region of 50–100 s^{-1} in many technical applications (nuclear reactor safety, explosion containment, crash problems, steel transformations, etc.). Precision testing at these strain rates already requires that stress-wave propagation phenomena be taken into account and therefore the use of the Hopkinson bar is a prerequisite; the MHB clearly allows a problem-free generation of the long duration pulses needed. When devices other than the Hopkinson bar are used to test at strain rates around 100 s^{-1}, the measured dynamic

mechanical properties will be affected by inaccuracies, especially as regards the initial yield strength and the fracture strength.

(2) The problems encountered in the standard Hopkinson bar regarding non-perfect contact and interface planarity during projectile–incident bar impact are avoided. The physical continuity of the pre-tensioned and incident bars of the MHB and the bending free working of the theta clamp ensure that the generated plane wave remains plane during propagation along the whole system without perturbations. This last characteristic allows to reliably record physical phenomena, such as initial yield peaks, flow curve oscillations due to phase transformations or other types of heterogeneity of the plastic flow.

(3) The diameter and the cross-section geometry of the MHB bar system can be modified easily. This possibility permits the adaptation of the MHB to the specific testing problem for a range of applications and industrial activities (nuclear reactor, automotive, aerospace, metallurgy fields, plastics, etc.).

(4) The MHB equipment possesses good versatility. By using the same supporting structure, the same hydraulic actuators and blocking device, etc., a variety of materials can be tested by simply changing the input and output bars in order to properly adjust the mechanical impedance of the bars with that of the specimen for obtaining the best recordable amplitudes of the incident, reflected and transmitted pulses.

4. Effects of the high strain rate on stress–strain curves of nuclear material in tension

(a) Effects on as-received austenitic and ferritic steels at room temperature

The effects of strain rate, increasing from 10^{-3} to $10^{3}\,s^{-1}$, on the stress–strain curves at room temperature of as-received austenitic stainless steels consist mainly in a marked increase of the stress at a given strain (strain rate hardening) and in a reduction of the uniform and fracture strains. Such phenomena are illustrated in figure 4 for the austenitic stainless steels AISI304L, AISI321, AISI316L, where the stress–strain curves at each strain rate show strain hardening.

The effects of strain rate increase, in the same range as above, on the stress–strain curves of ferritic steels, e.g. ASME537, also consist in a marked strain rate hardening but with practically no reduction of ductility, as illustrated in figure 5. The appearance of the upper and lower yield stress for the highest strain rate ($1330\,s^{-1}$), typical of the bcc metals, can also be observed, confirming the capability of the apparatus to reliably capture such plastic flow instabilities. The stress–strain curves at each strain rate clearly show strain hardening, too.

(b) Effects of high temperature on as-received austenitic and ferritic steels

The dynamic stress–strain curves of the same austenitic stainless steels mentioned above have been measured at high temperatures ranging from 100 to 950°C also in the strain rate range from 10^{-3} to $10^{3}\,s^{-1}$. At testing temperatures between 100 and 400°C, the dynamic stress–strain curves of these steels show both strain hardening and strain rate hardening. At temperatures ranging from 500 to 650°C, the dynamic stress–strain curves of austenitic stainless steels show a reduction of the uniform strain and strain rate softening, i.e. the stress at a given strain decreases with increasing strain rate. This behaviour is mainly attributed to the adiabatic conditions of dynamic loading, which become more accentuated at higher temperatures and render the thermal softening dominant, thus lowering the flow stresses at higher strain rates. At the same time, dynamic strain ageing (a diffusion-controlled phenomenon at elevated temperatures) may cause the rising of the flow stresses for the quasi-static loading. At testing temperatures from 750 to 950°C, a marked strain rate hardening is typically found, which is often associated to recrystallization phenomena [16,22].

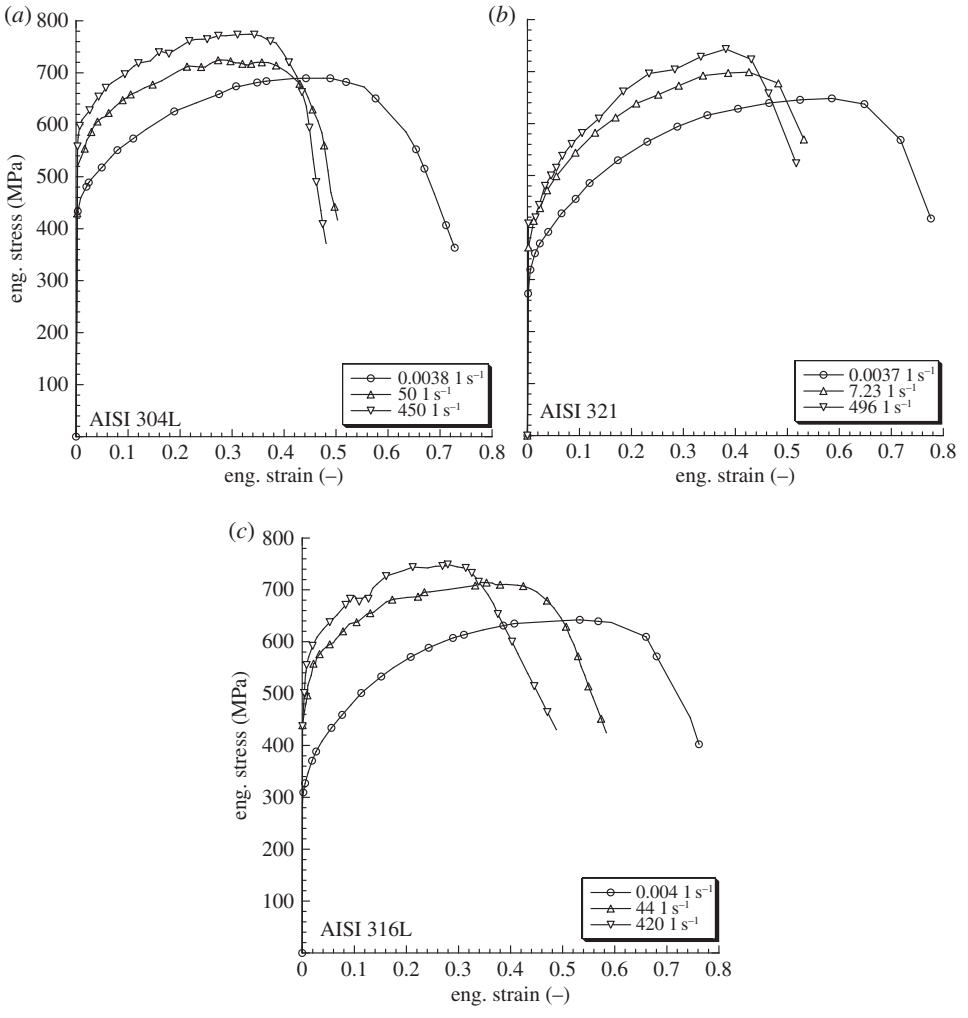

Figure 4. Stress–strain curves of austenitic stainless steels at room temperature: (*a*) AISI304L, (*b*) AISI 321 and (*c*) AISI 316L.

The dynamic flow curves of the ferritic steels also show the phenomenon of strain rate softening at higher temperatures [16,22].

(c) Effects of irradiation, high temperature and high strain rate on austenitic stainless steels

The dynamic stress–strain curves at room and high temperature (400, 500 and 550°C) of the austenitic stainless steels AISI316L, AISI316H, AISI304L and of the Nimonic Alloy Pe16, after irradiation in the high flux reactor (HFR) at JRC-Petten at the doses of 2 and 9.2 dpa, have been measured. An example from this extensive programme [9–13], regarding AISI316L steel, is reported in figure 6 [11].

From this figure, it is observed that the effects of the 9.2 dpa irradiation of AISI316L (comparison of the irradiated and the as-received material flow curves at the same strain rate) consist mainly in a strong increase of the flow stress at a given strain (damage hardening) and in a reduction of uniform and fracture strain. The dynamic flow curves at 550°C of this material irradiated to 9.2 dpa show a marked strain rate softening and reduction of the uniform and fracture strains [11].

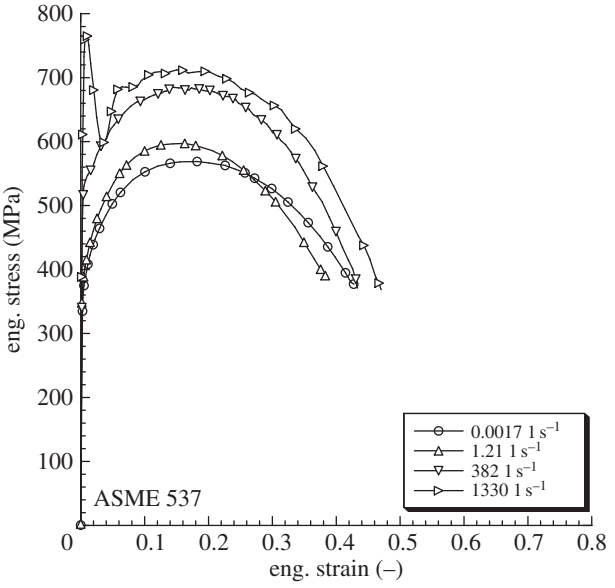

Figure 5. Stress–strain curves of ASME 537 ferritic steel at room temperature.

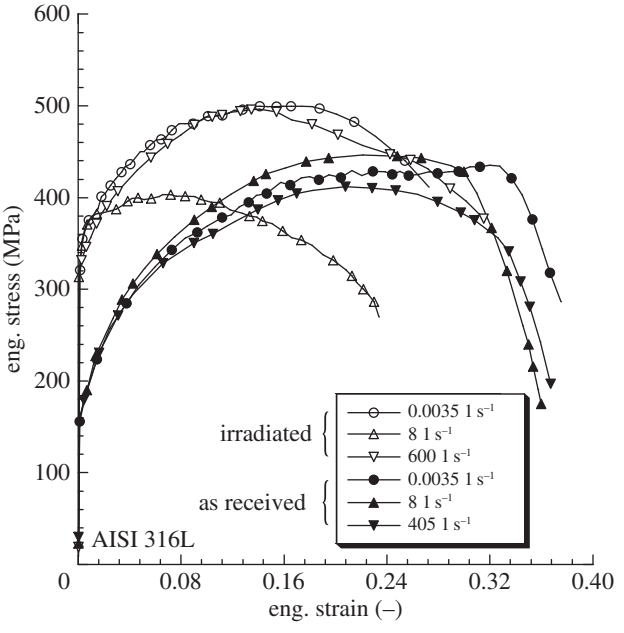

Figure 6. Stress–strain curves of irradiated (2 dpa) and as-received AISI316L steel measured at 550°C and at different strain rates.

(d) Effects of welding, high temperature and high strain rate on AISI316H stainless steel

The investigation regarding the comparison of the dynamic stress–strain curves at higher temperatures for AISI316L, AISI316H in as-received conditions, in welded conditions and heat-affected zone conditions is reported in [23]. Figure 7 shows the stress–strain curves of AISI316H stainless steel as base material, as weld material and as heat-affected zone material, tested at 400°C.

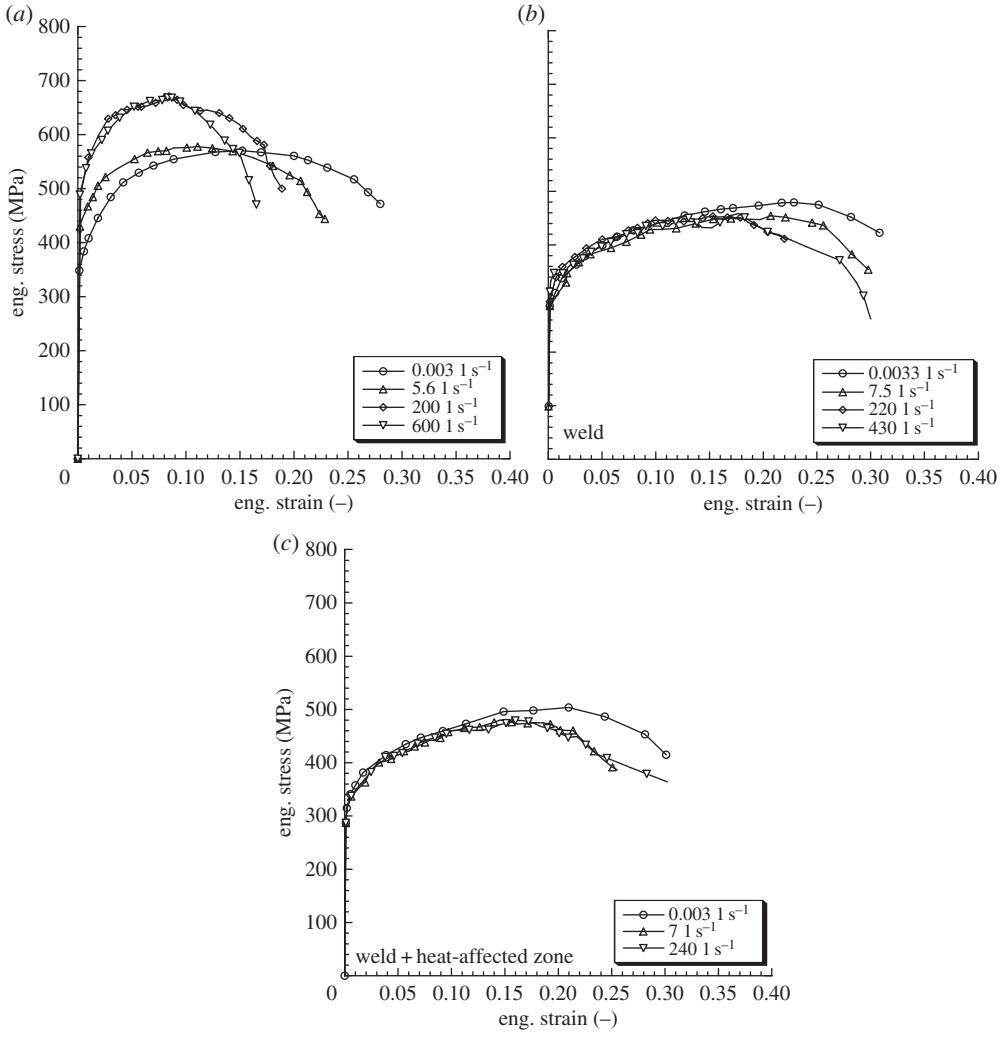

Figure 7. Stress versus strain curves of AIS316H steels at 400°C: (*a*) base material, (*b*) weld, (*c*) weld + HAZ.

As it can be observed, these curves indicate

(1) a substantial reduction in strength of the weld and weld + heat-affected zone materials with respect to the base one, with, however, no reduction in their ductility;
(2) a strain hardening and a strain rate hardening behaviour for the dynamic flow curves of the base material together with a marked reduction of the uniform and fracture strains; and
(3) a quite similar behaviour, i.e. a strain rate softening and some oscillations in the dynamic flow curves, for the weld and weld + heat-affected zone materials.

5. Irradiated austenitic steel AISI304L under high strain rate

As mentioned previously, this is a new and complete set of results and is presented for the first time. For the needs of this investigation, some austenitic structural steels have been irradiated at various reactors in order to study the evolution of their mechanical properties with respect to the irradiation damage rate, in particular under high deformation velocity.

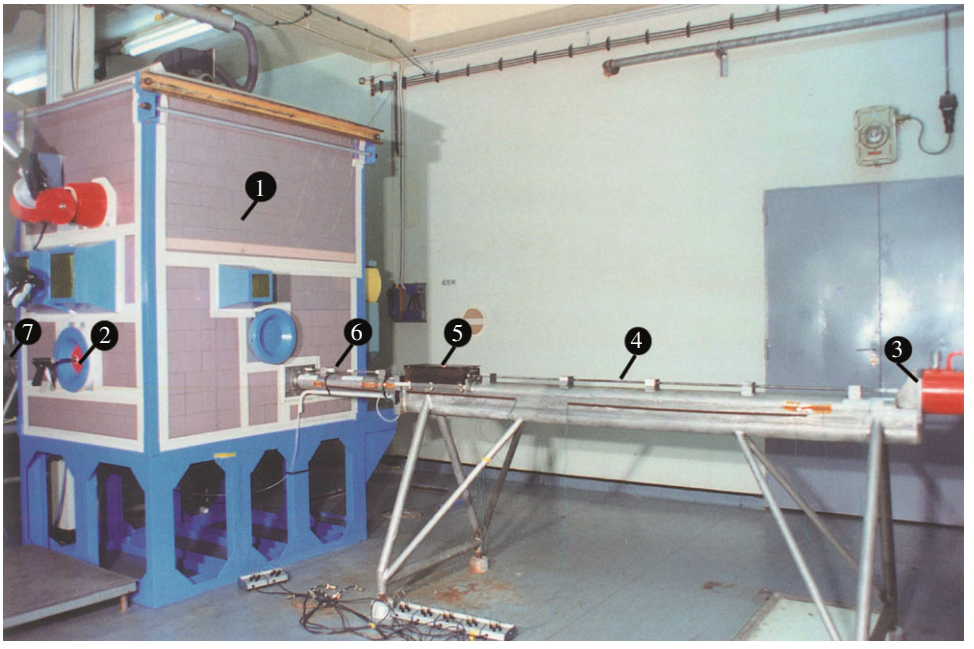

Figure 8. MHB set-up in hot cell for testing irradiated AISI304L stainless steel specimens: 1, hot cell; 2, manipulator; 3, hydraulic actuator; 4, pre-stressed bar; 5, blocking system; 6, input bar; 7, output bar. (Online version in colour.)

Two of these irradiations, called AUSTIN (Austenitic Steel IrradiatioN) 01 and 02, have used the HFR reactor at JRC-Petten. Specifically, 32 specimens of AISI304L have been subjected to a fluence of 2.1×10^{22} neutrons (n) cm^{-2} (instantaneous flux 0.887×10^{15} n cm^{-2} s^{-1}), for 1200 days of irradiation time with 45 HFR cycles at $500 \pm 20^{\circ}C$, reaching a dose of 30 displacements per atom (dpa).

The high strain rate tests have been performed by means of a MHB installed in a hot cell in the ESSOR reactor complex at Ispra, as shown in figure 8. Both the dynamic and the quasi-static tests were carried out at three different temperatures: 20, 400 and 550°C. The results of this experimental campaign on irradiated and as-received AISI304L specimens are reported in tables 1 and 2. The corresponding stress–strain diagrams are reported in figure 9*a*,*b*, respectively.

By observing figure 9*a*, it can be noted that at 20°C, as the strain rate increases, the flow stress at a given strain increases remarkably and the fracture strain decreases. At high temperature (400 and 550°C), one observes a very moderate increase in the flow stress and a small decrease of the fracture strain with increasing strain rates.

Figure 9*b* shows the main features of the mechanical behaviour of the irradiated material. It is seen that considerable strain rate hardening exists at the higher temperatures, while no strain rate sensitivity appears to be present at room temperature.

The comparison of the dynamic properties of the irradiated and the as-received material can be obtained from figure 9 and tables 1 and 2, and may be summarized as follows:

— the yield stress of the irradiated AISI304L steel, tested at room temperature and up to 550°C, is higher than that of the as-received material for all the strain rates examined. At room temperature, this increase varies between 55% for quasi-static and 7% for dynamic conditions, respectively;
— the ultimate tensile stress of the irradiated AISI304L is slightly higher than that of the as-received material for all strain rates and temperatures;
— the uniform strain of the irradiated material decreases with respect to that of the as-received material for all strain rates and temperatures examined; and

Table 1. Results on as-received specimens of AISI304L.

condition (°C)	strain rate (s^{-1})	yield stress (MPa)	UTS (MPa)	uniform strain (—)	eng. fracture stress (MPa)	fracture strain (—)
20	0.0038	435	689	0.442	363	0.729
	50	524	725	0.278	417	0.503
	450	582	774	0.333	372	0.48
400	0.0035	450	520	0.089	366	0.245
	50	437	511	0.033	252	0.269
	500	462	543	0.074	219	0.243
550	0.01	312	435	0.149	201	0.301
	126	342	444	0.088	276	0.284
	295	347	455	0.13	237	0.292
	671	362	463	0.108	207	0.326

Table 2. Results on irradiated specimens of AISI304L.

condition	strain rate (s^{-1})	yield stress (MPa)	UTS (MPa)	uniform strain (—)	eng. fracture stress (MPa)	fracture strain (—)
30 dpa 20°C	0.0038	686	849	0.346	703	0.489
	385	719	926	0.239	898	0.254
	399	512	791	0.250	784	0.268
	452	622	881	0.285	872	0.304
30 dpa 400°C	0.0040	408	483	0.077	376	0.207
	0.0040	377	453	0.100	352	0.242
	705	554	628	0.091	412	0.273
	600	469	583	0.109	376	0.311
	660	378	516	0.124	301	0.370
30 dpa 550°C	0.0039	330	405	0.054	373	0.099
	0.0038	389	432	0.028	411	0.051
	548	505	548	0.059	345	0.242
	688	360	471	0.129	278	0.363

— at room temperature, the fracture strain of the irradiated material decreases by about 50% with respect to that of the virgin material for all the strain rates examined. At the higher temperatures, a smaller such reduction is observed.

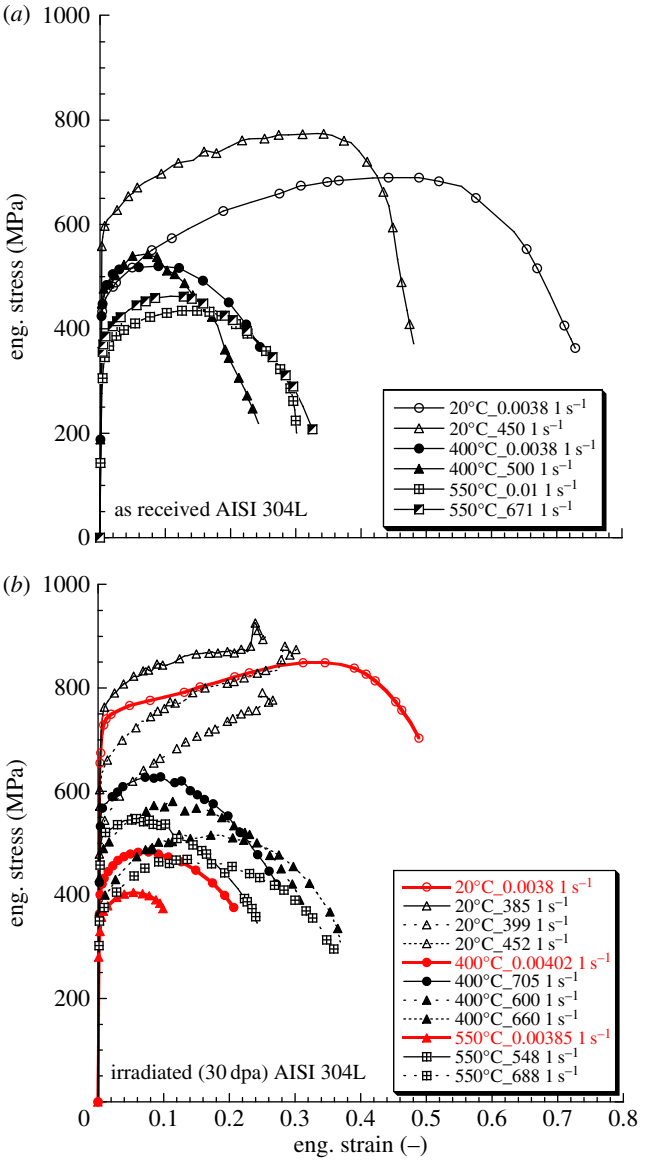

Figure 9. Stress–strain curves of (*a*) as-received and (*b*) irradiated AISI304L specimens. (Online version in colour.)

6. Large facilities for high strain rate

The need to test dynamically larger specimens and components has led to the development of the large Hopkinson bar facility (HOPLAB) of the JRC (figure 10). Its principle of operation is based on that shown in figure 2, where the pre-tensioned energy storage 'bar' is a cable, consisting of 32 steel strands, of 100 m length and 3200 mm^2 total cross-sectional area. In the current configuration of the HOPLAB, the incident and transmitter bars are solid bars of 72 mm diameter; the length of the incident bar is approximately 12 m and that of the transmitter bar 90 m. A rectangular force pulse of maximum amplitude of about 2.0 MN and of duration 40 ms can be potentially generated. Thus, with a maximum stroke of about 600 mm, this apparatus can bring to fracture very large specimens and components of ductile materials.

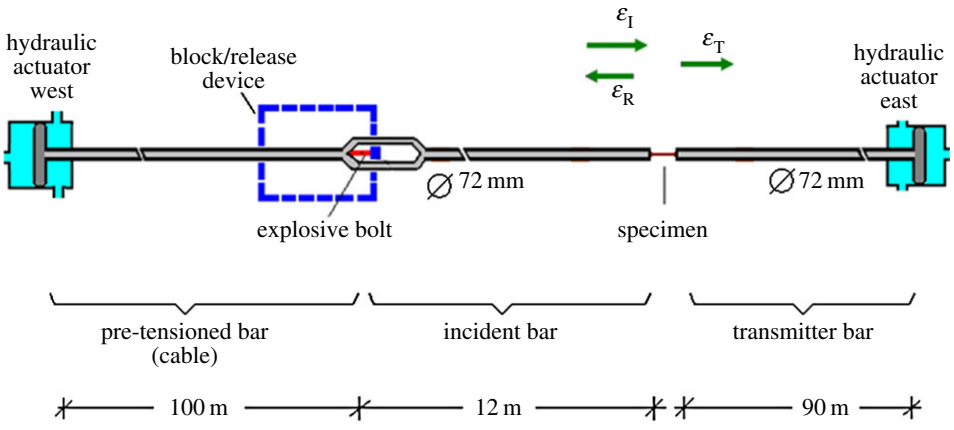

Figure 10. Schematic of large MHB for testing of large specimens. (Online version in colour.)

Clearly, this machine is more sophisticated in its operation and poses technical demands for the management of the enormous energy involved. As seen in figure 10, the configuration includes two large hydraulic actuators at the two outer extremes of the bars and a very strong blocking system. The static pre-tensioning of the cable is now resisted by and transmitted to the supporting structure through a large bolt made of brittle steel. The bolt has a weakened section with a circumferential notch and a hole, which is filled with explosive. When the desired level of pre-tensioning has been reached, the explosive is detonated causing the stretched bolt to fracture instantaneously. Thus, a tensile pulse is generated, as before, and travels down the incident bar. Of course, the mathematics of the analysis of the HOPLAB tests is fully analogous to that of the Hopkinson bar analysis.

Several dynamic testing campaigns have been conducted on large steel specimens in the frame of the Nuclear Reactor Safety programmes. The overall objective has always been the assessment of steel containment shells in case of severe dynamic loading, specifically owing to accidental explosions inside the reactor core causing high-pressure waves and impacts of projectiles.

One significant testing campaign has aimed to verify the specimen size effects on the dynamic mechanical properties of steels widely used in nuclear reactor structures. For the austenitic steel X6CrNiNb1810, experiments have been performed with ∅3, ∅9 and ∅30 mm cylindrical specimens, at room temperature and at 600°C, using the HOPLAB and smaller machines. The specimens were geometrically similar, as shown in figure 11. The detailed results of the testing campaign are reported in [16], where a major conclusion was that size effects at high strain rate must be principally sought in parameters of local deformation and at regions of strong strain gradients. In figure 12, typical dynamic stress–strain curves of the three specimens are shown for room temperature.

A second example of a very large specimen used to dynamically test real size weldings is depicted in figure 13. Finally, a case of large biaxial specimens of the ferritic steel 22NiMoCr37, tested at the HOPLAB in the frame of the EU project LISSAC [24], is shown in figure 14. Dynamic loading has been applied along one axis, while deformations have been constrained along the other. The elaborate nature of this cruciform specimen is to be noted; it has been constructed by electro-discharge machining and the finger-like bars serve to properly hold the central gauge region of the specimen of dimensions $80 \times 80 \times 4\,\mathrm{mm}^3$.

For history's sake, it is interesting to mention that the original design and configuration of this large MHB was founded on the concept of two MHBs aligned along the same axis, counteracting on a large specimen placed between them. The installation was composed of two equal arms, each one consisting of a cable of $3200\,\mathrm{mm}^2$ cross-sectional area and of 100 m length, whose far head was connected to a hydraulic actuator, whereas the central head was connected to the specimen

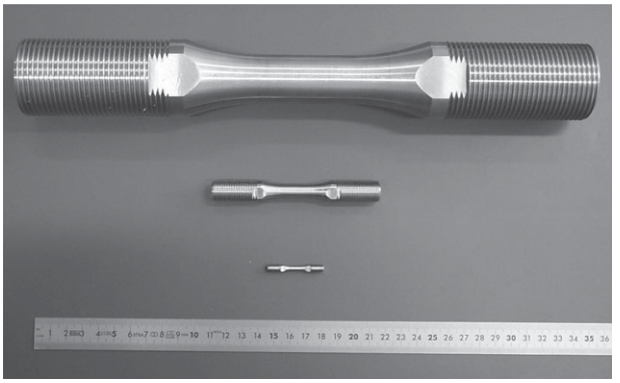

Figure 11. Specimen of 3, 9, 30 mm diameter for the study of size effect at high strain rate.

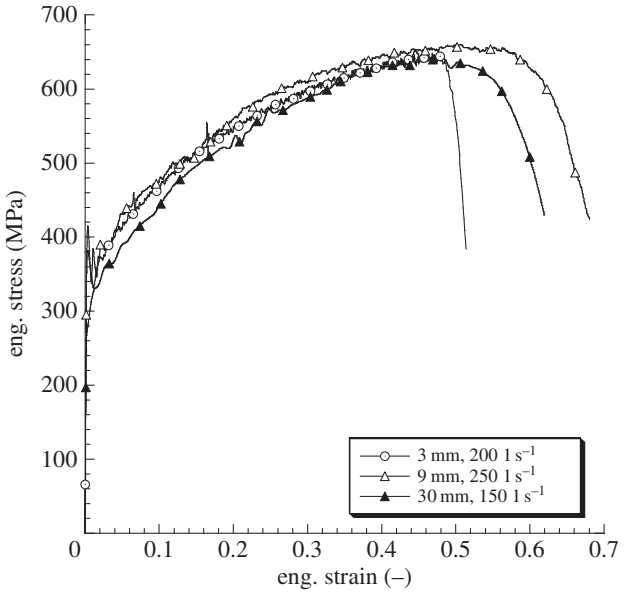

Figure 12. Stress–strain curves at room temperature of 3, 9, 30 mm diameter specimens of austenitic steel X6CrNiNb1810.

through a transmission rod and a cleave. The central head of the cable was also temporarily connected to the rigid supporting structure through the cross bar and the explosive bolts. The testing procedure included the blocking of the central heads of the cables, the static pre-tensioning of the cables, their sudden release by simultaneously fracturing the two explosive bolts, etc. This machine was successively transformed into a single MHB (figure 10) and was known for years as the large dynamic test facility (LDTF). It was employed with success in the field of automotive safety for a precise measurement of the load-displacement curves of crash energy absorbers and other structural components of cars involved in crash accidents [25,26], and it was successfully exploited as precision testing apparatus in support of the validation of computer codes for the design of dynamically loaded structures and for the advanced calibration of impacts rigs [27,28]. Finally, in the field of safety of civil engineering structures, where the large concrete aggregates impose the use of large specimens, this facility has already produced significant results [29–32] and its use in such applications is being further expanded. Today's HOPLAB facility is the refurbished and upgraded version of the LDTF.

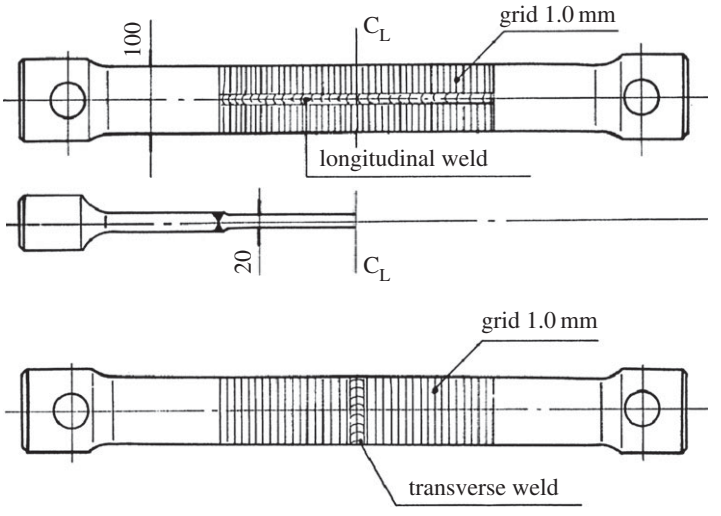

Figure 13. Specimen for the study of weld properties at high strain rate.

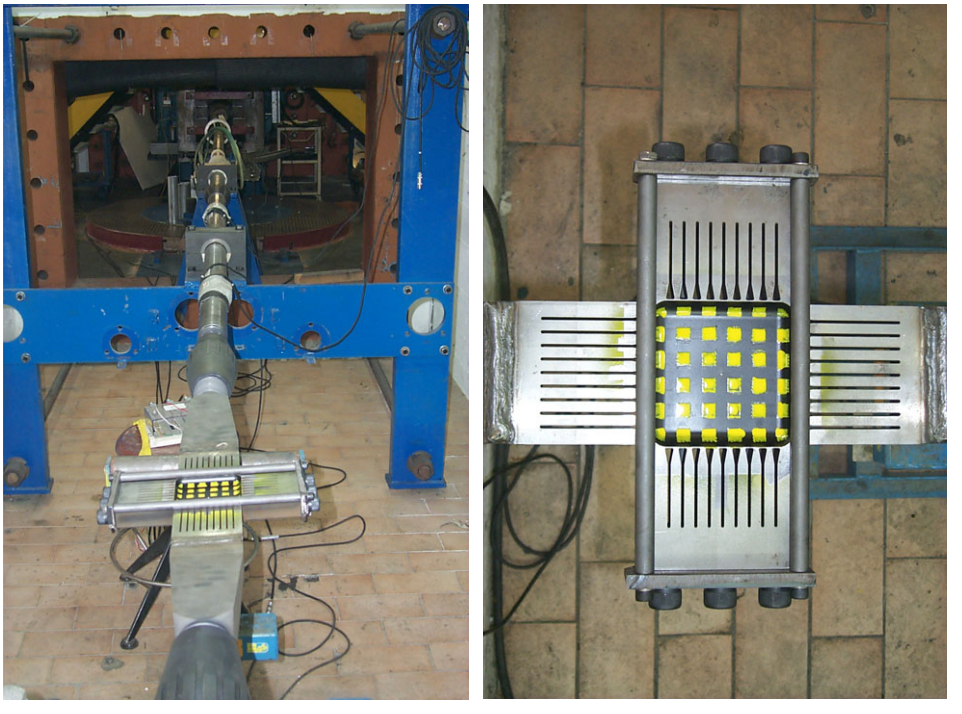

Figure 14. Large cruciform biaxial specimen tested dynamically at the HOPLAB. (Online version in colour.)

7. Conclusion

A qualitative and quantitative review has been made of the results obtained from the extensive dynamic testing of nuclear steels conducted in the frame of the Reactor Safety Programme at the JRC from 1971 to 2005. The review regards tensile properties and, in particular, the tensile stress–strain curves measured at high strain rate and at high temperature of several austenitic stainless

steels (AISI316L, AISI316H, AISI304, AISI321, X6CrNiNb1810) pre-damaged by irradiation, creep, low cycle fatigue and welding, and of a ferritic steel (ASME 537).

Central in this experimental activity has been the development and employment of a modified version of the Hopkinson bar in tension. This apparatus generates the pulse loading specimen by releasing the elastic energy stored in a pre-tensioned bar solidly connected to the incident bar, thus eliminating the use of the gas-gun and the striker. This presents a series of advantages, in particular the generation of long duration pulses, and has greatly facilitated the dynamic tensile testing of ductile materials. One such machine has even been installed in a hot cell and has allowed the testing of irradiated specimens. A large version of this MHB has also been constructed, where pulses of 2.0 MN amplitude and of 40 ms duration can be generated.

These apparatuses have allowed the production of a wealth of experimental data concerning the dynamic tensile behaviour of the above-mentioned nuclear steels. Some of their salient points are summarized below.

At room temperature, the dynamic stress–strain curves of the above as-received austenitic steels show strain rate hardening and reduction of ductility, whereas the dynamic stress–strain curves of the as-received ferritic steels show strain rate hardening and no reduction of ductility. As a consequence, at room temperature, the studied materials maintain nearly the same capability of absorbing energy both at static and at dynamic conditions. Strain rate hardening assures a stable response of the reactor structures to severe accident impact loading.

At temperatures ranging from 400 to 650°C, the dynamic stress–strain curves of the above austenitic and ferritic steels in as-received conditions show mild strain rate softening, reduction of ductility and oscillations along their flow curve.

An accentuation of the above degradation aspects of strain rate softening, reduction of ductility and instabilities characterize the dynamic stress–strain curves at temperatures between 400 and 550°C of the AISI316L and H, AISI304 irradiated at 2 and 9.2 dpa.

Finally, the dynamic stress–strain curves at high temperature of AISI316H and AISI304, pre-damaged only by creep and low cycle fatigue, show strain rate hardening and reduction of ductility. However, when the pre-damage consists of the superposition of low cycle fatigue and irradiation, the dynamic flow curves exhibit again strain rate softening and reduction of ductility.

Thus, it appears that at temperatures between 300 and 650°C, irradiation levels starting already from 2 dpa and other damaging effects from low cycle fatigue or from welding processes, cause phenomena of strain rate softening, instabilities and reduction of ductility to these nuclear steels.

This degradation of the mechanical properties raises several issues when the response and structural integrity of aged reactor structures to severe accident impact loading are to be evaluated. Countries depending on nuclear energy production are already faced with the problem of extending the life of aged nuclear reactors, and it is clear that the re-assessment of these plants shall require knowledge of the dynamic mechanical properties of aged reactor material taken directly from the reactor structures. All applications of the MHBs, especially the large Hopkinson bar and the hot cell Hopkinson bar, and the extensive body of data on damaged materials, reported above and in the open literature, shall play once more an important role in this re-assessment process.

Acknowledgements. The authors wish to remember that Mario Montagnani, as the references indicate, initiated and promoted the research described in this paper to which he gave a fundamental contribution with his ideas and enthusiasm from the early 1970s until 1990. The generous advice and encouragement in the early phases of development of the dynamic material properties laboratory at JRC-Ispra from Prof. J. D. Campbell, of Oxford University, and from Dr U. Lindholm, of the Southwest Research Institute in San Antonio Texas, are also kindly acknowledged.

References

1. Hopkinson B. 1914 A method of measuring the pressure in the deformation of high explosive by impacts of bullets. *Phil. Trans. R. Soc. Lond. A* **213**, 437–452. (doi:10.1098/rsta.1914.0010)

2. Davis RM. 1948 A critical study of the Hopkinson bar. *Phil. Trans. R. Soc. Lond. A* **240**, 375–457. (doi:10.1098/rsta.1948.0001)
3. Kolsky H. 1949 An investigation of the mechanical properties of materials at very high rates of loading. *Proc. Phys. Soc. B* **62**, 676–700. (doi:10.1088/0370-1301/62/11/302)
4. Montagnani M, Albertini C, Buzzi U, Forlani M. 1973 *Dispositif de contrainte a accumulation mecanique pour essais dinamique de traction*. Institut national de la propriete industrielle: Paris Brevet No. 74.17085. The Patent Office of London, Patent No. 1.473.683, 1974. Italian Patent No. 50008A.
5. Albertini C, Montagnani M. 1974 Testing techniques based on the Split Hopkinson bar. In *Inst. of Physics, Conf. Ser. No 21, Oxford, UK, 2–4 April 1974*, pp. 22–32. London, UK: Institute of Physics.
6. Albertini C, Montagnani M. 1976 Waves propagation effects on dynamic loading. *J. NED* **37**, 115–124. North Holland Publishing Company.
7. Albertini C, Montagnani M. 1977 *Dynamic Material Properties of Several Steels for Fast Breeder Reactors Safety Analysis*. EUR 5787EN.
8. Albertini C, Montagnani M. *Dynamic Mechanical Properties of the austenitic stainless steels used for the vessel models of Code validation tests*. EUR8705 ENCCGS(83)CONT-D164.
9. Albertini C, Del Grande A, Montagnani M. 1979 Effects of irradiation on the constitutive equations of austenitic stainless steels under dynamic loading. In *9th Int. Symp. on Effects of Radiation on Structural Materials, Richland, WA, 11–13 July 1978* (eds JA Sprague, D Kramer), pp. 546–556. ASTM STP 683. Philadelphia, PA: ASTM.
10. Albertini C, Del Grande A, Montagnani M. 1981 Dynamic mechanical properties of AISI 304L irradiated to 2.2 dpa. In *10th Int. Symp. on Effects of Radiation on Materials, Savannah, GA, 3–5 June 1980* (eds D Kramer, HR Brager, JS Perrin), pp. 431–442. ASTM STP 725. Philadelphia, PA: ASTM.
11. Albertini C, Del Grande A, Montagnani M. 1985 Mechanical properties at high strain rate of AISI 316L stainless steel irradiated to 9.2 dpa. In *12th Int. Symp. on the Effects of Radiation on Materials, ASTM, Williamsburg, VA, 18–20 June 1984* (eds FA Garner, JS Perrin), pp. 783–794. ASTM STP 870. Philadelphia, PA: ASTM.
12. Albertini C, Del Grande A, Montagnani M, Pachera A. 1987 Mechanical properties at low and high strain rates of PE 16 alloys irradiated to 9.2 dpa. In *13th Int. Symp. on Influence of Radiation on Material Properties, Seattle, WA, 23–25 June 1986* (eds FA Garner, CH Henager, N Igata), pp. 151–161. ASTM STP 956. Philadelphia, PA: ASTM.
13. Albertini C, Del Grande A, Iida K, Montagnani M, Pachera A, Forlani M. 1990 Residual tensile properties at low and high strain rate of AISI 316H pre-damaged by creep, low cycle fatigue and irradiation to 2 dpa. In *14th Int. Symp. on Influence of Radiation on Materials, Andover, MA, 27–29 June 1988* (eds NH Packan, RE Stoller, AS Kumar), pp. 387–403. ASTM STP 1046V.II. Philadelphia, PA: ASTM.
14. Albertini C, Boone PM, Montagnani M. 1985 Development of the Hopkinson bar for testing large specimens in tension. *Journal de Physique Colloques* **46**, C5, pp. 499–504.
15. Albertini C, Montagnani M, Pizzinato V. 1987 Specimen size and shape effects at high strain rate on the mode of yielding and flow of AISI 316. In *Impact 87 Int. Conf. on Impact Loading and Dynamic Behavior of Materials, Bremen, Germany, May 1987* (eds CY Chiem, HD Kunze, LW Meyer), pp. 461–468. Oberursel, Germany: DGM-Verlag.
16. Solomos G, Albertini C, Labibes K, Pizzinato V, Viaccoz B. 2004 Strain-rate effects in nuclear steels at room and higher temperatures. *Nucl. Eng. Des.* **229**, 139–149. (doi:10.1016/j.nucengdes.2003.10.006)
17. Albertini C, Labibes K, Montagnani M, Pizzinato V, Solomos G, Viaccoz B. 2000 Biaxial direct tensile tests in a large range of strain rates. results on a ferritic nuclear steel. *J. Phys. IV France* **10**, 161–166. (doi:10.1051/jp4:2000927)
18. Albertini C. 1997 Material properties for reactor pressure vessels and containment shells under dynamic loading. *J. Nucl. Eng. Des.* **174**, 135–141. (doi:10.1016/S0029-5493(97)00077-0)
19. Cadoni E, Dotta M, Forni D, Spaetig P. 2011 Strain-rate behavior in tension of the tempered martensitic reduced activation steel Eurofer97. *J. Nucl. Mat.* **414**, 360–366. (doi:10.1016/j.jnucmat.2011.05.002)
20. Cadoni E, Dotta M, Forni D, Tesio N, Albertini C. 2013 Mechanical behaviour of quenched and self-tempered reinforcing steel in tension under high strain rate. *Mat. Des.* **49**, 657–666. (doi:10.1016/j.matdes.2013.02.008)

21. Verheyden N, Montagnani M, Albertini C, Forlani M, Prosdocimi G. *Dispositif permettant de bloquer et de liberer brusquement une barre de test soumise a des efforts de traction et/ou de torsion*. European Patent 0 364 919 B1.
22. Albertini C, Eleiche AM, Montagnani M. 1989 The influence of the strain rate history on the stress–strain diagram of AISI316H at high temperatures. *Res. Mech.* **27**, 233–245.
23. Albertini C, Montagnani M. 1978 Effect of welding on dynamic response of austenitic stainless steel for nuclear applications. In *3rd Int. Sym. on Criteria for Preventing Service Failure in Welded Structures, Tokyo, Japan, 26–28 September 1978*. Tokyo, Japan: Japan Welding Society.
24. Krieg R. 2005 Failure strains and proposed limit strains for a reactor pressure vessel under severe accident conditions. *Nucl. Eng. Des.* **235**, 199–212. (doi:10.1016/j.nucengdes.2004.08.056)
25. Albertini C, Cadoni E, Labibes K. 1997 Precision measurements of vehicle crashworthiness by means of a large Hopkinson bar. *J. Phys. IV* **07**, C379–C384. (doi:10.1051/jp4:1997316)
26. Cadoni E, D'Aiuto F, Albertini C. 2009 Dynamic behaviour of advanced high strength steels used in the automobile structures. In *Proc. of 'DYMAT 2009', Brussels, Belgium, 7–11 September 2009*, pp. 135–141. Paris, France: EDP Sciences.
27. Albertini C, Cadoni E, Crutzen Y, Francocci P, Inzaghi A, Labibes K, Petrangeli A. 1995 Crashworthiness studies of thin sheet metal structures by means of a large Hopkinson bar; benefits for the calibration of impact rigs and validation of numerical crash simulation. In *Int. Crashworthiness and Design Symp., Valenciennes, France, 3–4 May 1995*, pp. 11–26.
28. Albertini C, Solomos G, Labibes K. 1999 *Precision measurement technique of loads and displacements over an automotive body during crash testing*. SAE Special publication SP-1434, 1999-01-0426. (doi:10.4271/1999-01-0426)
29. Albertini C, Cadoni E, Labibes K. 1999 Study of the mechanical properties of plain concrete under dynamic loading. *Exp. Mech.* **39**, 137–141. (doi:10.1007/BF02331117)
30. Cadoni E, Labibes K, Albertini C, Berra M, Giangrasso M. 2001 Strain-rate effect on the tensile behaviour of concrete at different relative humidity levels. *Mater. Struct.* **34**, 21–26. (doi:10.1007/BF02482196)
31. Cadoni E, Albertini C, Solomos G. 2006 Analysis of the concrete behaviour in tension at high strain rate by a modified Hopkinson bar in support of impact resistant structural design. *J. Phys. IV* **134**, 647–652. (doi:10.1051/jp4:2006134100)
32. Cadoni E, Solomos G, Albertini C. 2009 Mechanical characterisation of concrete in tension and compression at high strain rate using a modified Hopkinson bar. *Mag. Concrete Res.* **61**, 221–230. (doi:10.1680/macr.2006.00035)